Influence of Stereoregularity of Polypropylene on Miscibility with Ethylene−1-Hexene Copolymer

Masayuki Yamaguchi* and Hiroshi Miyata

Yokkaichi Research Laboratory, TOSOH Corporation, 1-8 Kasumi, Yokkaichi, Mie 510-8540, Japan

Received January 5, 1999; Revised Manuscript Received June 15, 1999

ABSTRACT: The influence of stereoregularity of polypropylene on the miscibility with the ethylene−1-hexene copolymer (EHR) whose 1-hexene content is 57 mol % was studied by means of viscoelastic measurements, electron microscopic observation, and so on. In this study, two types of polypropylenes were used; one is an isotactic polypropylene (iPP), and the other is a syndiotactic polypropylene (sPP). The sPP is immiscible with the EHR in both molten and solid states, whereas the iPP is miscible with the EHR in the amorphous region. The difference in the miscibility with the EHR between sPP and iPP depends on the chain stiffness.

Introduction

It is well-known that ethylene−1-butene copolymer, ethylene−1-hexene copolymer, and ethylene−1-octene copolymer, whose α-olefin content is above 10 mol %, are now commercially available owing to the recent development of metallocene catalysts. From an industrial point of view, these ethylene−α-olefin copolymers are attractive materials for a modifier of isotactic polypropylene (iPP) in an attempt to enhance the low-temperature toughness. Furthermore, the ethylene−α-olefin copolymers produced by metallocene catalysts are suitable for the study on the compatibility with iPP,[1−3] because the copolymers have narrow molecular weight distribution and short chain branching distribution which will affect the miscibility and/or compatibility.

Carriere et al.[1] found that interfacial tension between iPP and the ethylene−α-olefin copolymers depends on the species and the contents of α-olefin unit in the copolymers. According to them, the interfacial tension between iPP and an ethylene−α-olefin copolymer whose α-olefin unit is 1-butene, 1-pentene, and 1-octene is lower than that between iPP and an ethylene−propylene copolymer, when the density of the copolymers is around 870 kg/m^3. It was also found that the interfacial tension decreases with increasing the α-olefin content in the copolymers,[1,3] which has been also revealed by our rheological measurements for the binary blends composed of iPP and conventional branched polyethylenes.[4] These results suggest that morphology in the binary blends of iPP and an ethylene−α-olefin copolymer can be controlled by the selection of the copolymer. Moreover, we have studied the miscibility for the binary blends of iPP and a rubbery ethylene−1-hexene copolymer (EHR) whose 1-hexene content is 57.1 mol % in detail by means of viscoelastic measurements in both molten and solid states.[5] As a result, relaxation spectra for the blends in the molten state are intermediate between those for the individual pure components. Furthermore, the blend films show a single glass-relaxation process at the temperature between those of the individual pure components. The peak temperatures of the blends well agree with the predicted values by using the Fox equation. The results indicate that the iPP is miscible with the EHR in the molten state and in the amorphous region in the solid state. Moreover, according to recent studies, ethylene−1-butene copolymer,[6−10] ethylene−1-hexene copolymer,[5−7,11−13] and ethylene−1-octene copolymer,[7] whose α-olefin content is above 50 mol %, are found to be miscible with amorphous iPP chains, although the copolymer chains are not incorporated into the crystalline lattice of iPP.[6] The blend which is miscible in the amorphous region exhibits low brittle−ductile transition temperature[11] and hardly shows stress whitening.[10−12] Furthermore, the anisotropy of mechanical properties for the injection-molded products of the amorphous-miscible blends is less prominent than those of the immiscible blends.[13]

Not only ethylene−α-olefin copolymers but also various kinds of polypropylenes, such as syndiotactic polypropylene (sPP) and atactic polypropylene (aPP), have been produced by the metallocene catalysts. Both polypropylenes were also investigated on the miscibility with iPP.[14−16] According to them, both sPP and aPP with high molecular weight are immiscible with iPP.[15,16] These experimental results suggest that stereoregularity of a polypropylene will affect the miscibility with ethylene−α-olefin copolymers. In this study, the influence of the stereoregularity of a polypropylene on the miscibility and/or compatibility with the EHR whose 1-hexene content is 57.1 mol %, which was used in the preceding study,[5] was investigated. For the purpose, iPP and sPP produced by the metallocene catalyst were used.

Experimental Section

Polymer Synthesis. All polymers used were produced by metallocene catalysts. Dimethylsilylenebis(2,4-dimethylcyclopentadienyl)hafnium dichloride ($(Me_2Si(2,4\text{-}Me_2Cp)_2)HfCl_2$) and diphenylmethylidene(cyclopentadienyl 2,7-di-*tert*-butylfluorenyl)zirconium dichloride ($Ph_2C(Cp)(2,7\text{-}^tBuFlu)\ ZrCl_2$) were synthesized according to the procedures already reported.[17,18] Trimethylaluminum (TMA), triisobutylaluminum (TIBA), and dimethylanilinium tetrakis(pentafluorophenyl)-borate ($[Me_2PhNH]^+\ [B(C_6F_5)_4]^-$) were obtained from Tosoh Akzo Corp. Propylene and toluene were commercially obtained and purified according to the usual procedures. The iPP was

* Corresponding author. Phone +81-593-63-2643; fax +81-593-63-1659; e-mail m_yama@tosoh.co.jp.

10.1021/ma990004s CCC: $18.00
Published on Web 08/17/1999

Table 1. Molecular Characteristics of Polypropylenes

	stereoregularity (%)			molecular weights		
sample	*mm*	*mr*	*rr*	$M_n \times 10^{-5}$	$M_w \times 10^{-5}$	$M_z \times 10^{-5}$
iPP	98.2	1.4	0.4	2.1	4.1	6.9
sPP	1.8	6.6	91.6	1.1	1.5	2.0

synthesized using the silica-supported hafnium catalyst system which is prepared as follows: Silica (CARIACT 30, Fuji Silysia Chemical Ltd.) was heat-treated at 973 K under vacuum for 6 h. The calcinated silica (5 g) was dispersed in 60 mL of toluene containing 25 mmol of TMA. After stirring at room temperature for 1 h, the material was warmed to 353 K and stirred for 1 h. Then the solid part was separated by decantation and washed with toluene several times. This material (2.0 g) was mixed with 100 mL of toluene containing 0.80 mmol of TIBA, 0.10 mmol of $(Me_2Si(2,4\text{-}Me_2Cp)_2)HfCl_2$, and 0.50 mmol of $[Me_2PhNH]^+ [B(C_6F_5)_4]^-$. The mixture was stirred for 1 h, washed with toluene, and dried at room temperature under vacuum. The contents of Hf and B in the silica-supported catalyst were 0.048 mmol (Hf)/g (silica) and 0.18 mmol (B)/g (silica), respectively. Polymerization was carried out in a 2 L stainless steel autoclave equipped with a temperature controller and a magnetic stirrer. The autoclave was filled with 0.5 L of toluene containing 0.50 mmol of TIBA and 1 L of propylene. The catalyst solution (in toluene, 46.3 mg of the supported catalyst (0.0022 mmol of Hf) and 0.15 mmol of TIBA) was injected into the reactor. In this polymerization system, the Al/Hf molar ratio was 300. Polymerization was conducted at 303 K for 0.5 h. The polymerization was terminated by adding ethanol. After the autoclave was degassed, the precipitated polymer was filtrated, washed with ethanol for several times, and dried at 373 K under vacuum. The sPP was synthesized using the catalyst system composed of $Ph_2C(Cp)(2,7\text{-}^t\text{BuFlu})ZrCl_2$, $[Me_2PhNH]^+[B(C_6F_5)_4]^-$, and TIBA. Polymerization was carried out in a 5 L stainless steel autoclave. The autoclave was filled with 1 L of toluene and 1 L of propylene. The catalyst solution (in toluene, 0.0020 mmol of $Ph_2C(Cp)(2,7\text{-}^t\text{BuFlu})ZrCl_2$, 0.0024 mmol of $[Me_2PhNH]^+ [B(C_6F_5)_4]^-$, and 1.0 mmol of TIBA) was injected into the reactor. Polymerization was conducted at 313 K for 0.5 h. The obtained polymer solution was precipitated with ethanol. Then the precipitated polymer was filtrated, washed, and dried. The polymerization procedure for the EHR was described elsewhere.[19]

Molecular Characterization. The characteristics of the polypropylenes are listed in Table 1. The content of triads was calculated from the pentads which is determined by ^{13}C NMR. The number-, weight-, and *z*-average molecular weights were determined by means of simultaneous measurements of intrinsic viscosity and gel permeation chromatography using the universal calibration curve,[20] in which *o*-dichlorobenzene was used as the solvent. As shown in the table, the molecular weights of the iPP used in this study are higher than those of the iPP used in the preceding study[5] ($M_w = 1.36 \times 10^5$). The M_n, M_w, and M_z of the EHR are 1.4×10^5, 2.0×10^5, and 2.7×10^5, respectively. The 1-hexene content in the EHR is 57.1 mol %.[5] The EHR has no crystalline phase, because 1-hexene content is much enough to hinder the crystallization of ethylene unit.

Sample Preparation. A polypropylene and the EHR were mixed in a solution of hot xylene with a small amount of BHT (2,6-di-*tert*-butyl*p*-cresol) as a thermal stabilizer. The blend composition of the components in the polypropylene/EHR was 75/25 (w/w). The polypropylenes and the blends were melt pressed in a laboratory hot press at 473 K and at 10 MPa for 15 min. The samples quenched at 303 K were prepared for measurements. The thickness of the compression-molded samples was adjusted to suitable thickness for measurements.

Measurements. The melting temperature T_m and the heat of fusion Δh_F were measured using a Perkin-Elmer DSC-7 differential scanning calorimeter flushed with nitrogen. The samples of about 10 mg weight sealed in aluminum pans were heated from room temperature to 500 K at a scanning rate of 10 K/min. The weight fraction of crystallinity χ_c is calculated by the following equation

$$\chi_c = \frac{\Delta h_F}{\Delta h_F(100\%)} \tag{1}$$

where $\Delta h_F(100\%)$ is the heat of fusion for the perfect crystal: 210 J/g for iPP[21] and 157 J/g for sPP.[22]

Wide-angle X-ray diffraction (WAXD) measurements were performed at room temperature using a Mac Science MXP18 X-ray diffractmeter. Flat samples were mounted directly into the diffractmeter. The experiments were carried out using Cu Kα radiation operating at 40 kV and 150 mA at a scanning rate of 2°/min over 2θ (Bragg angle) range from 10° to 30°.

Morphology of the blend films was studied using a JEOL transmission electron microscope (TEM; model JEM-2000FX). The ultrathin films were sectioned into slices after being stained by ruthenium tetraoxide.

Oscillatory shear moduli, G' and G'', in the molten state were measured using a cone−plate type rheometer (Rheometrics dynamic stress rheometer SR-2000) in the angular frequency ω of 1.0×10^{-2} to 1.0×10^2 s^{-1}. The temperature ranged from 463 to 503 K for the iPP and the iPP/EHR and from 423 to 503 K for the sPP and the sPP/EHR. Measurements were carried out under nitrogen atmosphere in order to avoid thermooxidative degradation. The time−temperature superposition was applied to frequency dependence of oscillatory moduli at different temperatures in an attempt to determine the linear viscoelastic properties over a wide range of time scale.

The temperature dependence of oscillatory tensile moduli, E' and E'', in the solid state was measured from 150 to 450 K using a dynamic mechanical analyzer (Rheology Co., Ltd., DVE V-4). The frequency used was 10 Hz, and the heating rate was 2 K/min. The rectangular specimens, in which the width is 1 mm, the thickness is 0.5 mm, and the length is 20 mm, were used.

Table 2. Thermal Properties for the Samples

sample	T_m (K)	Δh_F (J/g)	χ_c (%)
iPP	438.3	103.0	49.0
iPP/EHR	438.1	79.5	37.9
sPP	405.7	48.0	30.6
sPP/EHR	405.7	38.9	24.8

Results

Morphology in the Solid State. Melting temperature T_m, heat of fusion Δh_F, and weight fraction of crystallinity χ_c of the polypropylenes and the blends are summarized in Table 2. As seen in the table, the melting temperatures of the blends are identical with those of the pure polypropylenes within the experimental error. The heat of fusion of the blends is about 75% of those of the corresponding pure polypropylenes.

WAXD studies were carried out in order to obtain much information on the crystalline level of the blends. The diffraction patterns have a broad amorphous background superimposed on several diffraction lines. The 2θ positions of the peaks for the blends are identical with those for the pure polypropylenes, indicating the EHR molecules are not incorporated into the crystalline lattice of polypropylenes. Furthermore, blending of the EHR has no effect on the crystalline form of the polypropylenes. Figure 1 exemplifies the WAXD profiles for the sPP and the sPP/EHR. It was found from the DSC and WAXD measurements that blending of the EHR has little effect on the crystallization process of both polypropylenes.

Figure 2 shows the temperature dependence of tensile storage moduli E' and loss moduli E'' for the blend films.

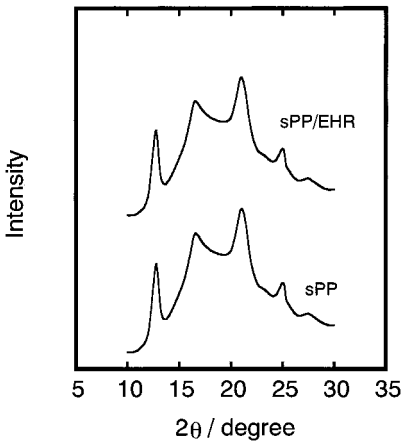

Figure 1. WAXD profiles for sPP and sPP/EHR.

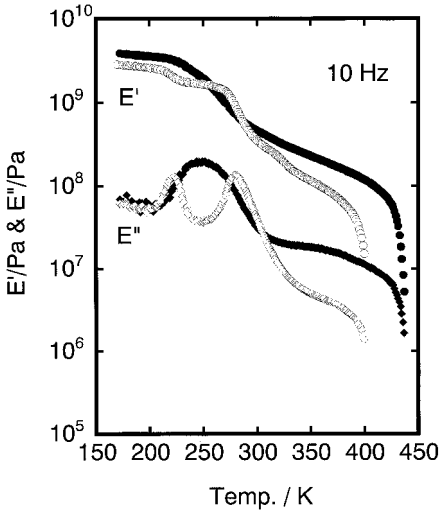

Figure 2. Temperature dependence of tensile storage modulus E' (circles) and tensile loss modulus E'' (diamonds) for iPP/EHR (closed symbols) and sPP/EHR (open symbols).

As seen in the figure, E' decreases with increasing the temperature and falls off sharply at the melting temperature. The magnitude of E' for the sPP/EHR is lower than that for the iPP/EHR, which is owing to the low degree of crystallinity for the sPP as shown in Table 2. Furthermore, the iPP/EHR shows only single relaxation peak in the E'' curve in the temperature range between 200 and 330 K, demonstrating EHR chains are incorporated into the amorphous region of the iPP. On the other hand, the sPP/EHR shows two separate peaks in the E'' curve, although molecular weight of the sPP is much lower than that of the iPP. Figure 3 shows the temperature dependence of E'' for the sPP, the EHR, and their blend in the temperature region between 200 and 350 K. The relaxation peaks in the figure are ascribed to the glass transition.[5,6] As seen in the figure, the peak temperature located in the lower temperature (about 230 K) for the blend is the same as that for the pure EHR, whereas the peak temperature located at the higher temperature (about 280 K) is the same as that for the pure sPP, demonstrating the sPP/EHR shows phase separation in the solid state.

Figure 4 shows electron micrographs of the blend films. As well-known, ruthenium tetraoxide preferentially stains the more amorphous phase; therefore, the white region denotes the polypropylene-rich phase, and

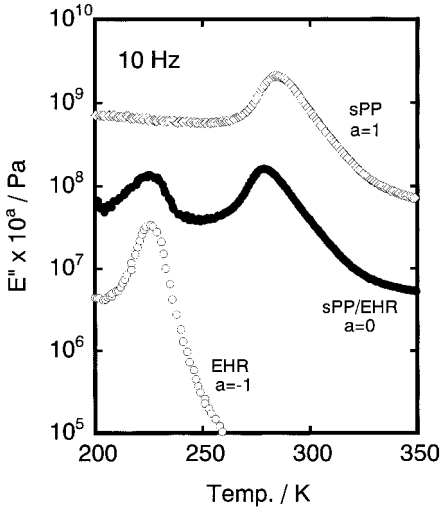

Figure 3. Temperature dependence of tensile loss modulus E'' for sPP (◇), sPP/EHR (●), and EHR (○).

the dark region denotes the EHR-rich phase. There is fairly homogeneous morphology in the iPP/EHR, whereas there is distinct microheterogeneous morphology in the sPP/EHR. The electron microscopic observation agrees well with the results of dynamic mechanical measurements: the iPP and the EHR are miscible in the amorphous region between the iPP lamellae; the sPP and the EHR are immiscible in both amorphous and crystalline regions. Moreover, the present results obtained for the iPP/EHR correspond to those obtained in the preceding study[5] in which the iPP with lower molecular weight was used.

Viscoelastic Properties in the Molten State. Figure 5 shows master curves of shear storage modulus G' and loss modulus G'' for the iPP and the sPP. The reference temperature is 463 K. The apparent activation energy of the iPP was 39 kJ/mol, and that of the sPP was about 53 kJ/mol, which are in good agreement with the values reported previously.[5,23,24] The zero-shear viscosity η_0 is determined by the following relation

$$\eta_0 = \lim_{\omega \to 0} \frac{G''}{\omega} \tag{2}$$

The η_0 of the sPP (1.5×10^4 Pa s) is closed to that of the iPP (2.0×10^4 Pa s), although the M_w of the iPP is much higher than that of the sPP. According to Eckstein et al.,[23] the difference in the unperturbed dimension of molecular chains affects the zero-shear viscosity η_0; that is, sPP is more expanded than iPP. Furthermore, a considerably large number of all-trans conformations of sPP in the molten state have been reported by Sozzani et al.[25] and Loos et al.,[26] which corresponds to the prediction by Suter and Flory.[27]

Moreover, it was found from Figure 5 that the magnitude of G' at the crossing point, that is, at the frequency of $\tan \delta = 1$, of the sPP is much larger than that of the iPP, even though the difference in the molecular weight distribution, as shown in Table 1, is considered. This result indicates that the rubbery plateau modulus G_N^0 of the sPP is higher than that of the iPP. Eckstein et al.[24] showed by their viscoelastic measurements that the rubbery plateau modulus G_N^0 of sPP (1.35×10^6 Pa) is much higher than that of iPP (4.27×10^5 Pa) at 463 K. They also showed that there

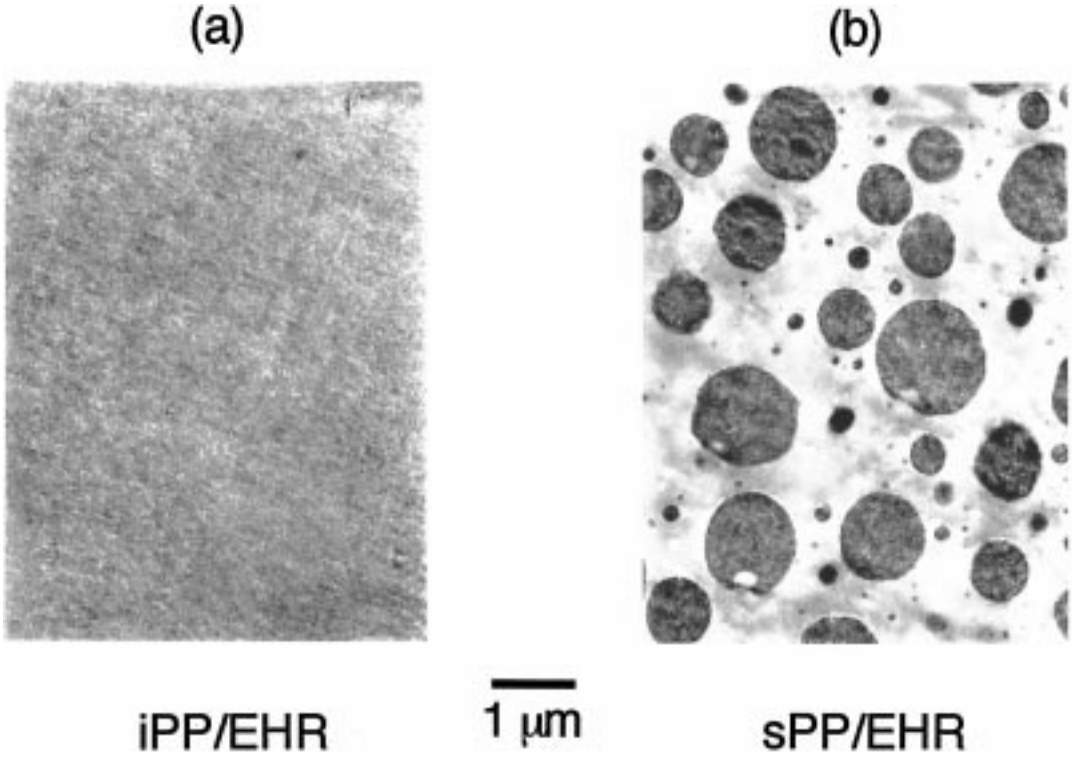

Figure 4. Transmission electron micrographs for (a) iPP/EHR and (b) sPP/EHR. The samples were stained with RuO_4.

is little difference in the density between sPP (762 kg/m^3) and iPP (766 kg/m^3) at the temperature. Therefore, the difference in G_N^0 is ascribed to the difference in average molecular weight between entanglement coupling points (M_e).

Figure 6 shows the master curve of oscillatory shear moduli for the blends in the molten state. The reference temperature is 463 K. The principle of time−temperature superposition was applicable to the frequency dependence of the oscillatory moduli for both blends, indicating the molecular aggregation state of the blends is stable over the entire experimental regions of frequency or temperature. As seen in Figure 6a, the slope of G'' is 1.0 and that of G' is closed to 2.0 for the iPP/EHR. Furthermore, the moduli for the iPP/EHR are intermediate between those for the individual pure components. These results indicate that entanglement slippage is the longest relaxation mechanism for the iPP/EHR. (The oscillatory moduli for the EHR and the rheological parameters in the terminal region for a miscible iPP/EHR have been described in detail in ref 5.) On the other hand, the sPP/EHR shows the "second plateau" in the G' curve at low-frequency region. The second plateau for the sPP/EHR is ascribed to the long time relaxation mechanism related to the microheterogeneous structure, demonstrating the sPP is immiscible with the EHR in the molten state. Thus, it can be concluded that morphology in the solid state for the blends of polypropylene and the EHR is decided by the miscibility in the molten state in the present study.

Discussion

Interfacial Tension between sPP and EHR. According to Palierne,[28] linear viscoelastic properties in the molten state for immiscible polymer blends are well expressed by a rheological emulsion model. Furthermore, the analysis can be used as a method to determine

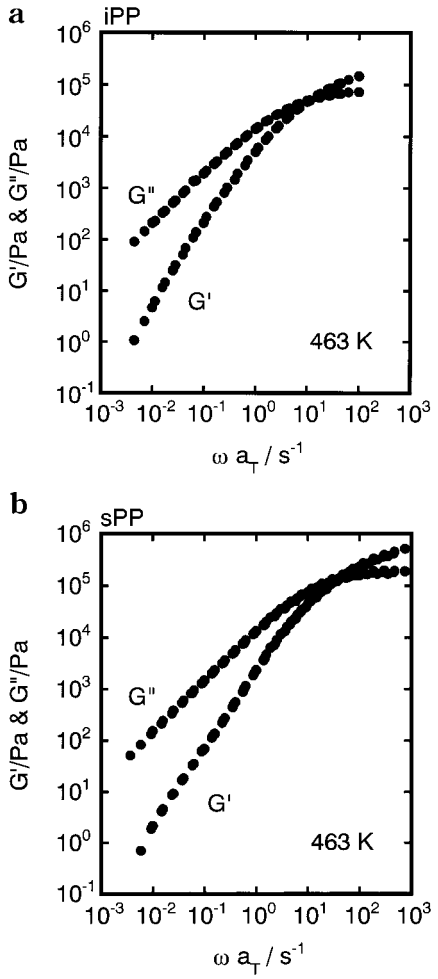

Figure 5. Master curves of shear storage modulus G' and shear loss modulus G'' for (a) iPP and (b) sPP. The reference temperature is 463 K.

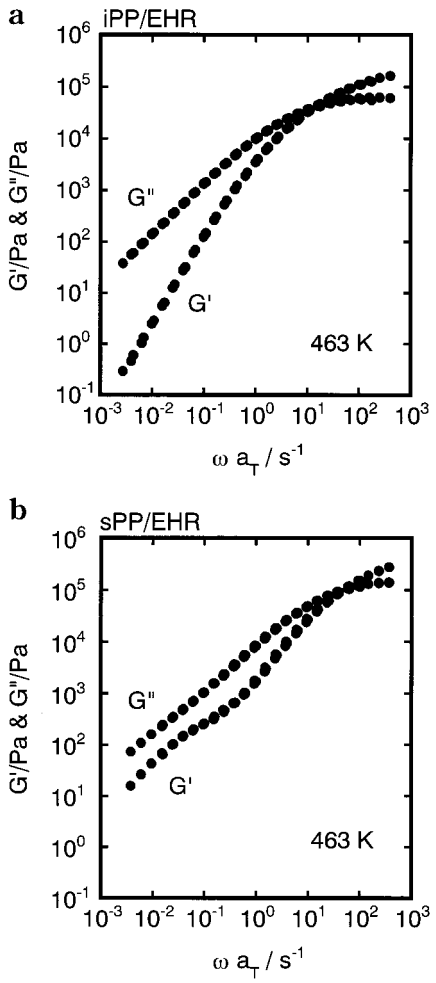

Figure 6. Master curves of shear storage modulus G' and shear loss modulus G'' for (a) iPP/EHR and (b) sPP/EHR. The reference temperature is 463 K.

the interfacial tension between two immiscible polymer melts.[4,28−30] The emulsion model is given as the following relation

$$G^*(\omega) = G_m^*(\omega)\frac{1 + 3\phi H(\omega)}{1 - 2\phi H(\omega)}$$

$$H(\omega) = [4(\gamma/R)\{2G_m^*(\omega) + 5G_d^*(\omega)\} + \{G_d^*(\omega) - G_m^*(\omega)\}\{16G_m^*(\omega) + 19G_d^*(\omega)\}]/[40(\gamma/R)\{G_m^*(\omega) + G_d^*(\omega)\} + \{2G_d^*(\omega) + 3G_m^*(\omega)\}\{16G_m^*(\omega) + 19G_d^*(\omega)\}] \quad (3)$$

where $G_d^*(\omega)$, $G_m^*(\omega)$, and $G^*(\omega)$ are the respective complex moduli of the dispersed phase, matrix, and blend at angular frequency ω; γ is the interfacial tension; and ϕ and R are the volume fraction and the volume average radius, respectively, of the dispersed phase.

Figure 7 compares the shear moduli calculated by the emulsion model and the experienced values for the sPP/EHR. The calculated values represented by solid lines well agree with the experimental results denoted by open circles. From the domain size R, which is estimated by Figure 4b, the interfacial tension between the sPP and the EHR is found to be 0.33 mN/m at 463 K. The value is smaller than that between iPP and the ethylene−propylene copolymer whose propylene content is 19.2 mol % (0.53 mN/m)[30] and that between iPP and the ethylene−1-butene copolymer whose 1-butene content is 6.4 mol % (1.0 mN/m).[4]

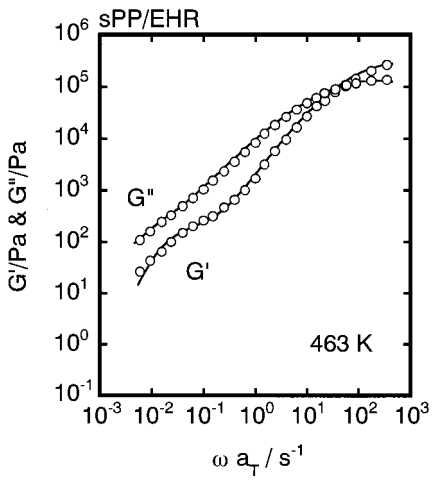

Figure 7. Comparison of calculated (solid lines) and experimental (open circles) oscillatory shear moduli for sPP/EHR.

Effect of Stereoregularity of Polypropylene on Miscibility with EHR. Recently, a theoretical approach on the miscibility of polyolefin blends has been developed intensively,[31−35] in which the experimental results[6,36−38] obtained by small-angle neutron scattering measurements were discussed. In these studies, it was pointed out that the difference in the chain stiffness, such as statistical segmental length and characteristic ratio, between the two polymers much affects the miscibility. Consequently, a pair of polyolefins tend to be immiscible when the difference in the statistical segmental length is prominent.

It was found from the present study that the iPP is miscible with the EHR, suggesting there is little difference in the chain stiffness between iPP and the EHR. On the other hand, the difference in the chain stiffness between sPP and the EHR will be prominent. As discussed above, the rubbery plateau modulus of the sPP is much higher than that of the iPP, indicating the statistical segmental length of polypropylene depends on the stereoregularity. According to Graessley and Edwards,[39] the plateau modulus G_N^0 is related with the statistical segmental length l by

$$\frac{G_N^0 l^3}{kT} \propto (\nu L l^2)^2 \quad (4)$$

where k is the Boltzmann constant, ν the number of chains per unit volume, and L the chain length. Following the relation, the statistical segmental length is proportional to G_N^0 when the product of ν and L is constant. Furthermore, both polypropylenes have the same monomer unit and show almost the same density at 463 K.[24] Therefore, the statistical segmental length of sPP is considered to be larger than that of iPP.

The effect of stereoregularity of polypropylene on the chain stiffness has been also demonstrated by Suter and Flory.[27] According to them, the characteristic ratio C_∞, which relates to the statistical segmental length l by eq 5, is greatest for sPP and decreases monotonically as the proportion of *meso* dyads increases.

$$C_\infty = l/l_0 \quad (5)$$

where l_0 is the average length of the main chain bonds.

Thus, the stereoregularity of polypropylene, which is responsible for G_N^0 and M_e, affects the miscibility with the EHR corresponding to their chain stiffness.

Conclusions

The influence of the stereoregularity of polypropylene on the miscibility with an ethylene−1-hexene copolymer (EHR) with 57.1 mol % of 1-hexene was studied. Syndiotactic polypropylene (sPP) whose rubbery plateau modulus is much higher than that of isotactic polypropylene (iPP) is immiscible with the EHR in the molten state. Consequently, the blend shows phase-separated morphology in the solid state. On the other hand, the iPP is miscible with the EHR in the molten state and in the amorphous region in the solid state. The difference in the miscibility with the EHR between sPP and iPP is associated with the chain stiffness which affects the rubbery plateau modulus.

References and Notes

(1) Carriere, C. J.; Silvis, H. C. *J. Appl. Polym. Sci.* **1997**, *66*, 1175−1181.
(2) Rana, D.; Lee, C. H.; Cho, K.; Lee, B. H.; Choe, S. *J. Appl. Polym. Sci.* **1998**, *69*, 2441−2450.
(3) Maier, R.-D.; Suhm, J.; Kressler, J.; Mülhaupt, R. *Polym. Bull.* **1998**, *40*, 337−344.
(4) Yamaguchi, M. *J. Appl. Polym. Sci.* **1998**, *70*, 457−463.
(5) Yamaguchi, M.; Miyata, H.; Nitta, K.; Masuda, T. *J. Appl. Polym. Sci.* **1997**, *63*, 467−474.
(6) Yamaguchi, M.; Miyata, H.; Nitta, K. *J. Appl. Polym. Sci.* **1996**, *62*, 87−97.
(7) Yamaguchi, M.; Nitta, K. *Rep. Polym. Phys. Prog.* **1996**, *39*, 457−458.
(8) Weimann, P. A.; Jones, T. D.; Hillmyer, M. A.; Bates, F. S.; Londono, J. D.; Melnichenko, Y.; Wignall, G. D.; Almdal, K. *Macromolecules* **1997**, *30*, 3650−3657.
(9) Kaneko, T.; Miyata, H.; Yamaguchi, M.; Akimoto, A. *Proceeding of FLEXPO'98, Houston, TX*, 1998.
(10) Thomann, Y.; Suhm, J.; Thomann, R.; Bar, G.; Maier, R.-D.; Mülhaupt, R. *Macromolecules* **1998**, *31*, 5441−5449.
(11) Yamaguchi, M.; Miyata, H.; Furukawa, H.; Akimoto, A. *Proceeding of MetCon '98 Worldwide Metallocene Conference,* Houston, June 1998.
(12) Yamaguchi, M.; Nitta, K. *Polym. Eng. Sci.* **1999**, *39*, 833−840.
(13) Yamaguchi, M.; Suzuki, K.; Miyata, H. *J. Polym. Sci., Polym. Phys. Ed.* **1999**, *37*, 701−713.
(14) Thomann, R.; Kressler, J.; Setz, S.; Wang, C.; Mülhaupt, R. *Polymer* **1996**, *37*, 2627−2634, 2635−2640.
(15) Maier, R.; Thomann, R.; Kressler, J.; Mülhaupt, R.; Rudolf, B. *J. Polym. Sci., Polym. Phys. Ed.* **1997**, *35*, 1135−1144.
(16) Silvestri, R.; Sgarzi, P. *Polymer* **1998**, *39*, 5871−5876.
(17) Mise, T.; Miya, S.; Yamazaki, H. *Chem. Lett.* **1989**, 1853−1856.
(18) Alt, H. G.; Zenk, R. *Organomet. Chem.* **1996**, *522*, 39−54.
(19) Miyata, H.; Yamaguchi, M.; Akimoto, A. *Proceeding of MetCon '96 Worldwide Metallocene Conference,* Houston, June 1996.
(20) Grubisic, Z.; Rempp, P.; Benoit, H. *J. Polym. Sci., Polym. Lett. Ed.* **1967**, *5*, 753−759.
(21) Wunderlich, B. *Macromolecular Physics*; Academic Press: New York, 1973.
(22) Balbontin, G.; Dainelli, D.; Galimberti, M.; Paganetto, G. *Makromol. Chem.* **1992**, *193*, 693−703.
(23) Eckstein, A.; Friedrich, C.; Lobbrecht, A.; Spitz, R.; Mülhaupt, R. *Acta Polym.* **1997**, *48*, 41−46.
(24) Eckstein, A.; Friedrich, C.; Suhm, J.; Friedrich, C.; Maier, R.-D.; Sassmannshausen, J.; Bochmann, M.; Mülhaupt, R. *Macromolecules* **1998**, *31*, 1335−1340.
(25) Sozzani, P.; Simonutti, R.; Galimberti, M. *Macromolecules* **1993**, *26*, 5782−5789.
(26) Loos, J.; Buhk, M.; Petermann, J.; Zoumis, K.; Kaminsky, W. *Polymer* **1996**, *37*, 387−391.
(27) Suter, U. W.; Flory, P. J. *Macromolecules* **1975**, *8*, 765−775.
(28) Palierne, J. F. *Rheol. Acta* **1990**, *29*, 204−214.
(29) Graebling, D.; Muller, R.; Palierne, J. F. *Macromolecules* **1993**, *26*, 320−329.
(30) Maeda, S.; Kamei, E. *J. Soc. Rheol., Jpn.* **1994**, *22*, 145−154.
(31) Bates, F. S.; Schulz, M. F.; Rosedale, J. H. *Macromolecules* **1992**, *25*, 5547−5550.
(32) Liu, A. J.; Fredrickson, G. H. *Macromolecules* **1992**, *25*, 5551−5553.
(33) Schweizer, K. S. *Macromolecules* **1993**, *26*, 6050−6067.
(34) Fredrickson, G. H.; Liu, A. J.; Bates, F. S. *Macromolecules* **1994**, *27*, 2503−2511.
(35) Freed, K. F.; Dudowicz, J. *Macromolecules* **1996**, *29*, 625−636.
(36) Krishnamoorti, R.; Graessley, W. W.; Balsara, N. P.; Lohse, D. J. *Macromolecules* **1994**, *27*, 3073−3081.
(37) Krishnamoorti, R.; Graessley, W. W.; Fetters, L. J.; Garner, R. T.; Lohse, D. J. *Macromolecules* **1995**, *28*, 1252−1259.
(38) Graessley, W. W.; Krishnamoorti, R.; Reichart, G. C.; Balsara, N. P.; Fetters, L. J.; Lohse, D. J. *Macromolecules* **1995**, *28*, 1260−1270.
(39) Graessley, W. W.; Edwards, S. F. *Polymer* **1981**, *22*, 1329−1334.

MA990004S